The Crystal Structures of Pyrope and Grossularite at Elevated Temperatures

E. P. Meagher

*Department of Geological Sciences, University of British Columbia,
Vancouver, British Columbia*

Abstract

Single crystal X-ray intensity data have been collected for a grossularite at 25°, 365° and 675°C and a pyrope at 25°, 350°, 550°, and 750°C. Anisotropic least-squares refinements reveal that the oxygen positional parameters remain approximately constant in grossularite but change in pyrope. Linear thermal expansion coefficients per 1°C $[(l_T - l_{25°})/(T - 25)/l_{25°}]$ for the mean interatomic distances Ca–O and Al–O in grossularite are 0.8×10^{-5} and 1.3×10^{-5}, respectively, while those from Mg–O and Al–O in pyrope are 1.3×10^{-5} and 0.8×10^{-5}, respectively. The Si–O interatomic distances do not increase significantly as a function of temperature.

In pyrope, with increasing temperature, the rigid SiO_4 tetrahedra rotate to allow the shared octahedral edge to lengthen at a greater rate than the unshared edge, thereby decreasing the octahedral bond angle strain. In grossularite the tetrahedra do not rotate, and the octahedral bond angle strain does not change. Structural changes in aluminum silicate garnets as a function of heating are compared to changes resulting from chemical substitution at the triangular dodecahedral site.

Introduction

The crystal structure of a variety of silicate garnets have been investigated at room temperature in the past fifty years. Among these are the determinations by Menzer (1926), Abrahams and Geller (1957), Zemann and Zemann (1961), Gibbs and Smith (1965), Euler and Bruce (1965), Prandl (1966), Novak and Meyer (1970) and Novak and Gibbs (1971). Novak and Gibbs (1971), who throroughly studied the crystal chemistry of the silicate garnets, discuss the response of the garnet structure to variations in chemistry and demonstrate the ability to predict the cell parameter as well as the bond lengths and angles given the composition of a particular silicate garnet.

As part of a study on high temperature crystal chemistry of silicate garnets, the crystal structures of pyrope and grossularite were determined from intensity data recorded at various elevated temperatures. It is hoped that, in addition to extending our understanding of the crystal chemistry of silicate minerals to high temperature, a study of this type will provide insight toward an understanding of the relationship of the crystal structures of minerals with their thermal expansions. Pyrope ($Mg_3Al_2Si_3O_{12}$) and grossularite ($Ca_3Al_2Si_3O_{12}$) were chosen for this study because they represent end-members with respect to the size of the eight-coordinated cation in the natural aluminum-silicate garnet series (Zemann, 1962).

Experimental

The grossularite here investigated is the one of near end-member composition (Table 1) used by Novak and Gibbs (1971). The pyrope was synthesized at 1300°C and 36 kbars in the presence of water by Dr. F. R. Boyd of the Geophysical Laboratory. The structure of this garnet was refined by Gibbs and Smith (1965) and subsequently re-investigated by Novak and Gibbs (1971).

The furnace used for the single crystal work is a modified version of one designed by Foit and Peacor (1967). The furnace, which requires flat-cone Weissenberg geometry, has been adapted to a Weissenberg camera for space group and cell-dimension work and to a manually-operated Supper Weissenberg diffractometer for single-crystal intensity data collection. Furnace temperatures have been calibrated with materials of known melting points and with a thermocouple in place of the sample. Temperatures given are believed accurate to ±15°C. Zero and upper level flat-cone Weissenberg photographs of both garnets were obtained at the temperature of the crystal structure determination, and systematic absences in each case were consistent with space group symmetry *Ia3d*.

The unit cell parameter for both garnets at room temperature was determined by a least-squares refinement of back-reflection Weissenberg data (Table 1).

TABLE 1. Crystal Data for Pyrope and Grossularite

PYROPE	GROSSULARITE
Locality	
Synthesized by F.R. Boyd, Geophysical Laboratory, Washington, D.C.	Asbestos,Quebec
Composition	
$Mg_{3.00}Al_{2.00}Si_{3.00}O_{12}$	$Ca_{2.96}Mn_{0.04}Al_{1.95}Fe_{0.05}Si_3O_{12}$*
Calculated density	
3.53 gm./c.c.	3.62 gm./c.c.

Cell parameters

This study		
$25^\circ C$ 11.456(2)** Å	25°	11.846(2) Å
	365°	11.880(2)
Skinner (1956) [†]	675°	11.917(4)
$25^\circ C$ 11.459 Å		
350° 11.490		
550° 11.507		
750° 11.530		

* Novak and Gibbs (1971).
** Number in parentheses refers to one estimated standard deviation.
† Interpolated values from Skinner (1956) data. Estimated errors are ± 0.001.

The 11.456(2) Å cell edge determined for pyrope at 25°C compares favorably with 11.459 Å determined for a synthetic pyrope by Skinner (1956). The cell parameters determined by Skinner (1956) to a temperature of 758°C were interpolated for use in this investigation and are listed in Table 1. The cell parameters for grossularite at elevated temperatures were determined from Weissenberg film data utilizing a specially designed cassette. The cassette was constructed so that it can be dismantled without disturbing the furnace in order that the crystal alignment can be carried out by standard oscillation techniques before the Weissenberg photograph is recorded. The cell parameter for grossularite at elevated temperatures was determined from a least-squares refinement of the Weissenberg data corrected for absorption by the Nelson-Riley method (Nelson and Riley, 1945).

For intensity measurements the crystals were placed in tapered fused-silica glass capillaries. The grossularite crystal was cylindrical in shape with dimensions 0.11 × 0.07 mm. The pyrope crystal was equidimensional and 0.06 mm in diameter. Three dimensional single-crystal intensity data were collected utilizing flat-cone geometry on a manual Weissenberg scintillation counter diffractometer. Zr-filtered Mo$K\alpha$ radiation was used along with a pulse-height discriminator. Symmetry non-equivalent reflections of $\sin\theta \leq 0.5$ were scanned and traced on a strip chart recorder. Relative intensities were deter-

mined with an integration planimeter and corrected for Lorentz and polarization factors. Intensity data were collected at 25°, 350°, 550°, and 750°C for pyrope and 25°, 365°, and 675°C for grossularite. Following collection of data at high temperatures, intensity data were collected a second time at room temperature for both crystals. For each crystal a number of symmetry equivalent reflections were recorded to assess absorption errors. The differential absorption was considered negligible for both crystals, and corrections were not applied.

Refinements

Full matrix least-squares refinements were carried out using a modified version of ORFLS (Busing, Martin, and Levy, 1962). Scattering curves for neutral atoms were obtained from Doyle and Turner (1968) and starting positional and thermal parameters were obtained from Novak and Gibbs (1971). In the initial cycles of refinement a scale factor, the oxygen positions, and the isotropic temperature factors were varied. The weighting scheme of Cruickshank (1965) was used and adjusted for each refinement in order to yield constant values of $\langle w(Fo - Sc \cdot Fc)\rangle$ in equally populated groups of increasing Fo where Fo is the observed amplitude of the reflection, Fc the calculated amplitude, Sc the scale factor and w the weight assigned to each reflection. Upon convergence of the isotropic refinement the temperature factors were converted to the anisotropic form and the refinement continued. For both garnets, the anisotropic thermal parameters for the octahedral-site atom were statistically isotropic at all temperatures; therefore, the final cycle of refinement was carried out with an isotropic thermal parameter for this site. The refined positional parameters, weighted residual factors (wR), and the isotropic equivalents of the anisotropic temperature factors are given in Table 2 along with the positional parameters determined at room temperature by Novak and Gibbs (1971). The refined positional parameters of oxygen for the preheated garnets at 25°C were statistically identical to those determined at 25°C following the high temperature runs. The anisotropic temperature factor coefficients are given in Table 3, and the final observed and calculated structure amplitudes are listed in Table 4. Because of the small crystal sizes, a large number of reflections were too weak to be observed. These reflections were not included in the refinements nor in Table 4.

The interatomic distances and angles and their es-

TABLE 2.   Positional Parameters, Isotropic Temperature Factors*, and Weighted R-Factors for Pyrope and Grossularite

		x	y	z	B_0	B_X	B_{Al}**	B_{Si}	R†
PYROPE									
Novak & Gibbs (1971)	25°	0.0329(1)††	0.0502(1)	0.6534(1)	0.50(2)	0.79(3)	0.40(2)	0.19(2)	0.090
This Study	25°	0.0328(4)	0.0503(4)	0.6534(5)	0.47(11)	0.93(20)	0.40(6)	0.29(11)	0.021
	350°	0.0335(5)	0.0499(5)	0.6534(5)	0.95(13)	1.37(25)	0.71(7)	0.48(13)	0.018
	550°	0.0331(4)	0.0493(4)	0.6536(4)	0.89(9)	1.96(14)	0.75(6)	0.63(8)	0.019
	750°	0.0332(6)	0.0489(5)	0.6535(5)	1.53(11)	2.30(21)	1.12(7)	0.74(9)	0.023
GROSSULARITE									
Novak & Gibbs (1971)	25°	0.0381(1)	0.0449(1)	0.6514(1)	0.76(2)	0.61(1)	0.66(2)	0.56(2)	0.046
This Study	25°	0.0380(5)	0.0447(5)	0.6512(4)	0.37(9)	0.39(10)	0.40(6)	0.30(11)	0.024
	365°	0.0384(5)	0.0449(5)	0.6512(4)	0.81(10)	0.87(10)	0.63(6)	0.81(11)	0.026
	675°	0.0381(5)	0.0450(5)	0.6515(4)	1.12(9)	1.17(10)	0.94(6)	1.00(11)	0.029

```
*    Isotropic equivalents of the anisotropic temperature factors, Hamilton (1959).
**   Refined isotropically.
†    Weighted R-factor where R = (Σw (Fo - Fc)²/Σw Fo²).
††   Number in parentheses refers to one estimated standard deviation.
```

timated standard errors were calculated with the program ORFFE (Busing, Martin, and Levy, 1964) and are listed in Tables 5 and 6 respectively. The interatomic distances given are the distances between mean atomic positions and are not corrected for thermal displacements since the correlation between thermal displacements of the atoms in the garnet structure is not known.

The increase of interatomic distance with temperature can be conveniently described by a linear thermal expansion coefficient defined as:

$$\alpha = \frac{1}{l_{25°}} \frac{(l_T - l_{25°})}{(T - 25°)}$$

where l equals the interatomic distance. The value $(l_T - l_{25°})/(T-25°)$ in this paper represents the slope determined by linear regression of temperature $versus$ interatomic distances.

Discussion

The general structural formula for garnet can be written in the notation of Geller (1967) as: $\{X_3\}$ $[Y_2]$ (Z_3) O_{12} where $\{\ \ \}$ refers to the eight-coordinated triangular dodecahedral site, $[\ \ ]$ refers to the six-coordinated octahedral site, and $(\ \ )$ to the tetrahedral site (Fig. 1). For the more common natural end-member silicate garnets X refers to the divalent cations Ca, Mn, Fe^{2+}, Mg; Y refers to the trivalent cations Al, Cr, Fe^{3+}; and Z refers to Si. The details of the garnet structure have been adequately described by previous authors (*e.g.,* Abrahams and Geller, 1958; Gibbs and Smith, 1965) and will not be

repeated here. All the cations occupy special positions, and the crystal structure of a garnet is defined by its cell edge and its oxygen positional parameters.

In the aluminum silicate garnets $\{X_3\}$ $[Al_2]$ (Si_3) O_{12} the radius of the X-cation has a pronounced effect on the details of the structure (Novak and Gibbs, 1971). As a result, the pyrope and grossularite structures contrast most strongly and, as shown here and in Meagher (1973), respond very differently to in-

TABLE 3.   Anisotropic Temperature Factor Tensor Values for Pyrope and Grossularite*

		β_{11}	β_{22}	β_{33}	β_{12}	β_{13}	β_{23}
PYROPE							
25°C	Mg	72(59)**	231(100)	231	0	0	65(69)
	Si	38(41)	38	87(59)	0	0	0
	O	158(44)	38(33)	73(41)	14(34)	−10(9)	31(32)
350°C	Mg	179(80)	300(121)	300	0	0	34(81)
	Si	65(50)	65	140(69)	0	0	0
	O	223(54)	217(44)	99(44)	−8(37)	21(21)	−27(34)
550°C	Mg	112(45)	536(89)	536	0	0	168(62)
	Si	177(33)	177	2(37)	0	0	0
	O	147(35)	176(36)	182(38)	−3(30)	−60(19)	33(29)
750°C	Mg	194(54)	552(104)	552	0	0	156(70)
	Si	146(34)	146	127(45)	0	0	0
	O	288(44)	323(45)	252(42)	3(37)	−59(26)	−15(35)
GROSSULARITE							
25°C	Ca	73(40)	68(38)	68	0	0	6(28)
	Si	14(53)	14	135(54)	0	0	0
	O	77(35)	32(36)	89(39)	−45(30)	−35(26)	9(32)
365°C	Ca	56(33)	203(39)	203	0	0	16(30)
	Si	207(57)	207	8(48)	0	0	0
	O	151(39)	119(39)	161(42)	−17(32)	−9(30)	1(33)
675°C	Ca	89(35)	264(43)	264	0	0	0.5(30)
	Si	209(57)	209	110(51)	0	0	0
	O	233(35)	208(34)	148(31)	−8(33)	2(30)	21(30)

```
* Values reported are X 10⁵. The coefficients are of the form (β₁₁h² + ----------
  2β₁₂ hk + -------------).
** Number in parentheses refers to one estimated standard deviation.
```

TABLE 4. Observed and Calculated Structure Factors for Pyrope and Grossularite

GROSSULARITE

h k l	25°C Fo	25°C Fe	365°C Fo	365°C Fc	675°C Fo	675°C Fc
4 0 0	200·3	200·9	197·3	197·2	196·5	194·7
8 0 0	232·9	233·9	224·5	222·0	215·8	217·4
12 0 0					36·7	33·8
16 0 0	105·3	103·7	87·5	88·0	77·4	76·5
4 2 0	190·0	-188·4	186·0	-185·9	181·1	-184·2
6 2 0	38·9	33·8			36·9	35·7
10 2 0	63·8	-65·7	56·7	-58·3	55·0	-56·2
12 2 0	102·7	-102·4	93·1	-91·9		
4 4 0	65·4	-62·2	62·5	-59·6	62·4	-60·2
6 4 0	166·3	167·0	161·1	159·4	153·8	156·2
8 4 0	134·8	132·2	127·2	126·8	122·8	122·8
10 4 0	119·6	120·4	111·3	108·7	102·6	102·0
14 4 0	86·0	85·8	74·0	71·2	65·5	63·2
16 4 0	59·3	60·5	49·4	52·2	46·7	46·2
10 6 0	37·0	-37·1	26·6	-29·9	29·6	-27·7
12 6 0	93·4	-91·0	84·2	-78·8	75·3	-72·7
8 8 0	200·7	206·4	193·1	190·1	178·9	180·5
12 8 0	78·8	77·0	68·5	66·4	57·4	56·7
12 10 0	78·9	-76·8	67·8	-63·3	58·9	-56·6
6 1 1	91·0	91·6	95·9	92·5	91·4	89·7
5 2 1	62·8	-60·9	60·7	-58·7	60·7	-57·9
4 3 1	59·6	58·7	60·9	57·4	60·8	56·6
7 4 1	31·7	34·9	32·0	32·9	32·8	32·3
9 4 1	42·9	45·9	43·4	42·9	40·9	40·8
6 5 1	18·7	20·6	20·0	21·3	19·2	19·6
8 5 1	29·5	31·8	27·2	30·3	30·0	29·6
7 6 1	26·3	26·3	23·6	24·3	24·4	23·3
4 2 2	87·6	90·7	85·6	90·3	85·7	89·3
12 2 2	118·5	120·2	111·0	109·8	103·2	104·0
3 3 2	55·6	-50·7	53·4	-51·0	53·3	-50·7
5 3 2	65·5	61·3	63·6	59·0	61·1	57·8
9 3 2	21·9	23·6	21·3	19·6	18·9	17·4
6 4 2	156·7	157·6	147·5	151·9	145·0	148·0
8 4 2	128·4	-128·0	118·9	-119·2	117·2	-115·6
10 4 2	113·7	114·1	104·2	105·4	98·0	97·3
14 4 2	98·8	101·6	87·5	87·5	77·9	78·2
16 4 2	84·2	-80·4	65·5	-65·6	60·2	-58·8
5 5 2	41·3	-38·6	36·4	-34·3	35·1	-32·6
8 6 2	24·2	-26·0	22·8	-22·7	23·3	-22·3
12 6 2	64·7	63·7	58·6	57·4	54·3	53·8
7 7 2	30·2	31·2	28·4	26·6	22·3	23·8
12 8 2	90·9	89·7	77·3	75·1	70·9	69·3
12 10 2	74·4	76·9	66·8	65·4	60·7	58·6
6 3 3	23·4	-20·8	24·4	-22·6	18·2	-21·0
5 4 3	20·7	-20·3	18·6	-20·2	18·8	-19·3
6 5 3	25·2	25·2	22·3	22·9	21·0	22·3
8 5 3	46·8	-48·5	42·6	-44·0	40·7	-42·7
11 6 3			30·8	-32·3	29·9	-28·8
8 7 3	28·8	30·3	26·3	27·4	25·2	26·2
4 4 4	210·3	-209·5	198·6	-200·4	192·3	-197·6
12 4 4	79·0	-81·2	67·5	-68·1	63·5	-64·3
7 5 4	32·0	30·2	28·7	28·0	24·2	27·0
6 6 4	117·6	116·5	110·2	109·8	104·2	105·0
8 6 4	111·6	110·3	103·7	100·6	95·8	95·5
10 6 4	80·4	81·0	72·5	73·0	66·2	67·6
14 6 4	62·0	58·9	53·0	50·5	47·3	45·0
11 7 4	27·1	-26·3			23·4	-22·0
8 8 4	85·7	85·5	80·0	78·1		
10 8 4	94·8	-99·4	86·1	-85·7	76·6	-78·9
14 8 4	77·5	-76·0	66·0	-59·9	52·8	-51·8
10 10 4	80·5	83·7	68·8	71·5	61·2	65·0
7 6 5	25·6	-26·2	26·9	-24·5	21·3	-22·6
13 8 5	31·1	-26·5				
12 6 6	75·5	74·4	65·2	66·4	61·3	60·9
9 7 6	33·3	-32·7	27·4	-27·4		
12 8 6	83·5	85·3	71·4	69·6	62·5	63·3
9 9 6	32·8	-31·0	30·0	-27·1	26·3	-25·2
8 8 8	174·4	178·0	151·9	153·6	139·3	139·7
12 8 8	72·5	70·8	59·2	58·6	50·0	50·0

PYROPE

h k l	25° Fo	25° Fc	350°C Fo	350°C Fc	550°C Fo	550°C Fc	750°C Fo	750°C Fc
4 0 0	172·4	172·2	172·4	170·8	175·5	173·8	172·0	171·0
8 0 0	177·2	177·2	173·0	172·6	166·4	165·6	164·2	164·3
16 0 0	67·1	66·4	54·3	54·6	48·9	48·5	45·9	46·5
4 2 0	129·4	-130·8	132·6	-130·7	126·2	-127·7	128·8	-128·2
6 2 0	55·2	52·6	54·3	51·7	53·2	53 1	53·8	51·1
10 2 0	45·6	-44·9	42·0	-42·2	37·8	-38·3	36·7	-35·9
12 2 0	68·0	-69·4	66·7	-66·6	61·2	-61·3	59·0	-59·2
4 4 0	41·6	-41·0	41·6	-39·9	39·6	-38·7	39·2	-38·0
6 4 0	147·2	148·0	142·2	142·1	137·2	136·9	132·4	132·5
8 4 0	107·3	108·5	104·2	103·0	100·9	100·7	98·2	97·0
10 4 0	92·5	93·5	85·4	84·1	80·2	79·0	74·7	74·4
14 4 0	51·7	50·8	43·9	45·0	41·0	38·5	36·5	36·7
12 6 0	55·3	-53·1	51·6	-49·4	43·3	-42·3	45·0	-42·4
8 8 0	159·7	158·8	148·6	147·9	138·8	137·6	132·6	130·7
12 8 0	56·7	54·0	52·9	49·6	47·9	47·0	45·4	41·7
12 10 0			37·6	-38·3	32·6	-31·6	31·1	-31·2
2 1 1	17·9	17·7						
6 1 1	66·5	65·0			68·2	66·0	63·0	62·1
10 1 1	32·7	33·1	31·9	31·6	31·9	31·1	31·3	29·5
4 3 1	57·2	54·6	54·9	53·4	55·4	54·1	51·2	52·3
6 3 1	22·8	-21·8			21·8	-20·9	21·9	-21·2
7 4 1	30·3	-29·8	28·9	29·7	29·5	28·5	27·2	27·0
9 4 1	36·0	38·5	33·5	-36·1	33·8	-35·6	32·6	-32·2
4 2 2	64·3	67·9			61·3	65·0	62·6	64·4
12 2 2	100·2	102·5	94·3	94·3	90·6	91·3	84·2	84·1
6 4 2	136·0	136·0	129·5	132·8	126·2	130·0	123·9	126·0
8 4 2	88·4	-90·6	86·1	-85·8	84·8	-83·7	83·0	-81·8
10 4 2	89·3	91·4	83·1	84·1	82·4	82·4	76·7	76·0
14 4 2	70·2	73·5	64·3	64·4	60·9	62·6	54·2	54·0
5 5 2	21·8	-19·0						
12 6 2	50·8	50·4						
12 8 2	61·0	59·8						
2 3 3	87·4	-82·6	82·4	-81·3	83·7	-81·7	82·0	-79·6
6 5 3	37·0	35·1	36·6	34·8	36·4	35·4	31·6	34·1
8 5 3	44·5	-43·7	40·4	-40·9	38·8	-40·1	34·2	-36·0
11 6 3	23·3	-20·9						
4 4 4	148·2	-146·7	140·0	-140·5	138·0	-137·1	135·3	-135·4
12 4 4	43·7	-43·4						
7 5 4	34·4	34·5	30·6	31·6	31·3	32·5	26·9	29·6
6 6 4	96·6	95·3	89·1	91·4	90·0	88·2	83·8	85·2
8 6 4	71·1	71·3	65·8	69·1	62·9	62·0	61·0	61·7
10 6 4	64·0	65·2	61·1	60·6	56·7	56·4	50·5	52·6
14 6 4	47·0	43·9	36·4	37·2	36·0	35·2	30·9	31·0
8 8 4	73·4	74·0	68·2	67·8	65·5	64·7		
10 8 4	70·0	-73·7	70·2	-66·2	58·5	-59·0	55·5	-55·1
10 10 4	67·7	67·6	58·3	59·6			49·4	48·8
2 1 5	41·3	-39·9			39·7	-36·0	36·4	-34·4
8 1 5	29·4	-31·8	29·6	-30·4	32·6	-30·9	26·0	-28·7
3 2 5	37·4	34·9	35·7	33·3	33·4	32·0	28·8	30·2
7 1 6	39·1	-41·9	35·9	-38·9	37·9	-41·5	35·9	-38·5
12 6 6	60·9	56·4	51·6	51·2	47·9	46·5	41·7	42·6
12 8 6	60·5	57·6	48·2	49·0	46·4	44·9	41·9	41·0
9 9 6	43·1	-40·3	37·0	-36·3	39·7	-37·7	32·0	-32·1
8 8 6	124·6	124·5	112·1	110·2				
8 8 8	125·1	125·4	112·1	110·6	107·4	106·1	99·8	98·2
12 8 8					41·0	39·3	32·9	33·7

TABLE 5. Interatomic Distances for Pyrope and Grossularite*

PYROPE		Novak & Gibbs (1971) 25°C	This study 25°C	350°C	550°C	750°C	GROSSULARITE		Novak & Gibbs (1971) 25°C	This study 25°C	365°C	675°C
				About Si						About Si		
Si-O	4	1.634(1)*Å	1.635(5)Å	1.633(6)Å	1.634(5)Å	1.636(6)Å	Si-O	4	1.645(1)Å	1.647(5)Å	1.649(6)Å	1.654(6)Å
O(1)-O(2)	2	2.494(2)	2.495(11)	2.499(11)	2 492(10)	2.495(12)	O(1)-O(2)	2	2.567(2)	2.569(10)	2.578(11)	2.580(10)
O(1)-O(3)	4	2.751(3)	2.752(9)	2.746(10)	2.753(9)	2.756(10)	O(1)-O(3)	4	2.745(1)	2.747(9)	2.752(10)	2.760(10)
Mean O-O		2.665	2.666	2.664	2.666	2 669	Mean O-O		2.686	2.688	2.694	2.700
				About Al						About Al		
Al-O	6	1.886(1)	1.887(5)	1.893(6)	1.895(5)	1.897(6)	Al-O	6	1.924(1)	1.921(5)	1.929(5)	1.937(5)
O(1)-O(4)	6	2.617(3)	2.618(5)	2.635(10)	2.637(8)	2.643(10)	O(1)-O(4)	6	2.751(2)	2.751(9)	2.766(9)	2.775(9)
O(1)-O(5)	6	2.716(3)	2.719(9)	2.718(10)	2.722(8)	2.721(10)	O(1)-O(5)	6	2.686(2)	2.681(9)	2.690(9)	2.705(9)
Mean		2.667	2.669	2.677	2.680	2.682	Mean O-O		2.721	2.716	2.728	2.740
				About Mg						About Ca		
Mg(1)-O(4)	4	2.196(2)	2.197(6)	2.208(7)	2.205(5)	2.210(7)	Ca(1)-O(4)	4	2.319(1)	2.319(5)	2.330(5)	2.333(6)
Mg(2)-O(4)	4	2.342(2)	2.341(5)	2.354(6)	2.364(5)	2.373(6)	Ca(2)-O(4)	4	2.491(1)	2.492(6)	2.499(6)	2.505(6)
Mean Mg-O		2.269	2.269	2.281	2.285	2 292	Mean Ca-O		2.405	2.406	2.415	2.419
O(1)-O(2)	2	2.494(3)	2.495(11)	2.499(12)	2.492(9)	2.495(12)	O(1)-O(2)	2	2 567(2)	2.569(10)	2.578(10)	2.580(9)
O(1)-O(4)	4	2.617(3)	2.618(8)	2.635(9)	2.637(8)	2.643(10)	O(1)-O(4)	4	2.756(2)	2.751(8)	2.763(8)	2.775(7)
O(4)-O(6)	4	2.709(3)	2.706(10)	2.729(11)	2.734(9)	2.748(13)	O(4)-O(6)	4	2.973(2)	2.979(12)	2.989(12)	2.989(11)
O(1)-O(7)	4	3.306(1)	3.307(4)	3.318(4)	3.321(4)	3.328(4)	O(1)-O(7)	4	3.450(1)	3.452(4)	3.462(4)	3.470(3)
O(4)-O(7)	2	2.782(3)	2.781(11)	2.785(12)	2.806(10)	2.816(13)	O(4)-O(7)	2	2.866(2)	2.867(9)	2.876(9)	2.883(9)
O(7)-O(8)	2	3.825(3)	3.823(9)	3.852(10)	3.861(9)	3.877(12)	O(7)-O(8)	2	4.121(2)	4 123(12)	4.138(12)	4.145(11)
Mean O-O		2.929	2.929	2.944	2.949	2 958	Mean O-O		3.101	3.103	3.113	3.120
Mean O-O cube			2.654	2.669	2.673	2.682	Mean O-O cube			2.816	2.826	2.832

* Number in parentheses refers to one estimated standard deviation.

creasing temperature. The positional parameters (Table 2) show no significant shift of the oxygen positions in grossularite up to a temperature of 675°C, whereas in pyrope the **y** fractional coordinate decreases with increasing temperature.

Silicate Tetrahedron

The Si–O interatomic distance shows no significant lengthening upon heating. In grossularite, the Si–O distance increases slightly more than one standard error over the temperature range 25°–675° and the regression coefficient d (Si–O)/dT is greater than zero only at the 0.20 confidence level. In pyrope there is essentially no increase up to 750°C. The tetrahedral O–Si–O angles likewise show no variation beyond

one standard error in either garnet (Table 6). The resistance of the Si-tetrahedron to increase in size with heating has been observed in other orthosilicates (*cf* Smyth and Hazen, 1973; Brown and Prewitt, 1973).

In pyrope, although the silicate tetrahedron does not appear to change in size or shape with heating, it does rotate about the $\bar{4}$ axis which passes through its center. To express the rotation of the tetrahedron, Born and Zemann (1964) defined a positional angle, herein noted γ,[1] as the smaller of two angles between the tetrahedral O–O edge normal to the $\bar{4}$ axis and the two crystallographic axes normal to the $\bar{4}$ axis. The

---

[1] Born and Zemann use the notation, α, for this angle.

TABLE 6. Interatomic Angles for Pyrope and Grossularite*

PYROPE		25°C**	25°C	This Study 350°C	550°C	750°C	GROSSULARITE		25°C**	This Study 25°	365°C	675°C
				About Si						About Si		
O(1)-Si-O(2)	2	99.52°(9)*	99.50°(41)	99.84°(46)	99.35°(36)	99.37°(46)	O(1)-Si-O(2)	2	102.53(8)	102.7(3)	102.7(4)	102.5(4)
O(1)-Si-O(3)	4	114.67(9)	114.68(22)	114.49(25)	114.76(20)	114.75(25)	O(1)-Si-O(3)	4	113.05(4)	112.9(2)	113.0(2)	113.1(2)
				About Al						About Al		
O(1)-Al-O(4)	6	87.87(6)	87.81(22)	88.20(23)	88.19(22)	88.33(27)	O(1)-Al-O(4)	6	91.46(5)	91.6(2)	91.6(2)	91.5(3)
O(1)-Al-O(5)	6	92.13(6)	92.19(22)	91.78(23)	91.81(20)	91.67(28)	O(1)-Al-O(5)	6	88.54(5)	88.4(2)	88.4(2)	88.6(3)
				About Mg						About Ca		
O(1)-Mg-O(2)	2	69.20(7)	69.23(24)	68.90(27)	68.81(25)	68.73(29)	O(1)-Ca-O(2)	2	67.20(6)	67.3(3)	67.2(3)	67.2(3)
O(1)-Mg-O(4)	4	70.34(6)	70.48(23)	70.60(25)	70.42(24)	70.33(28)	O(1)-Ca-O(4)	4	69.84(4)	69,5(2)	69.7(3)	69.9(3)
O(4)-Mg-O(6)	4	73.22(6)	73.15(21)	73.40(23)	73.43(19)	73.60(25)	O(4)-Ca-O(6)	4	76.28(6)	76.6(2)	76.4(2)	76.2(2)
O(4)-Mg-O(7)	2	72.86(7)	72.88(26)	72.53(29)	72.81(23)	72.78(32)	O(4)-Ca-O(7)	2	70.27(6)	70.2(2)	70.2(2)	70.3(2)
O(1)-Mg-O(7)	4	93.47(7)	93.50(14)	93.27(16)	93.18(14)	93.08(18)	O(1)-Ca-O(7)	4	91.61(4)	91.6(2)	91.6(2)	91.6(3)
O(7)-Mg-O(8)	2	109.46(7)	109.45(25)	109.80(27)	109.53(23)	109.54(31)	O(7)-Ca-O(8)	2	111.66(6)	111.7(2)	111.7(2)	111.7(2)

* Number in parentheses refers to one estimated standard deviation
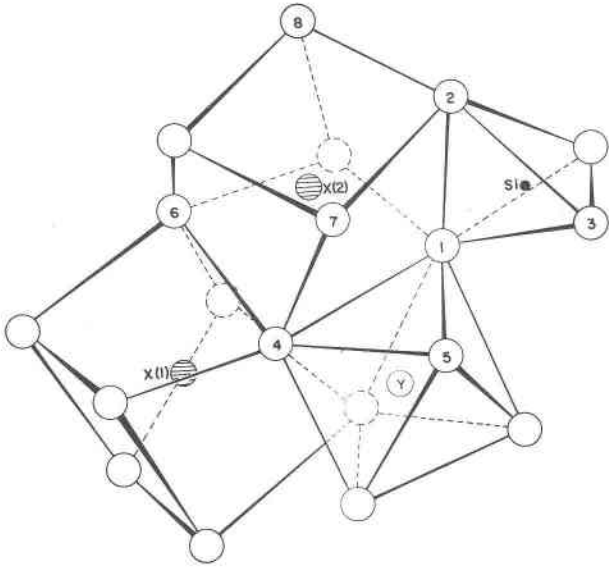** Novak and Gibbs (1971)

FIG. 1. A portion of the garnet structure (after Novak and Gibbs, 1971) showing numbering of atoms.
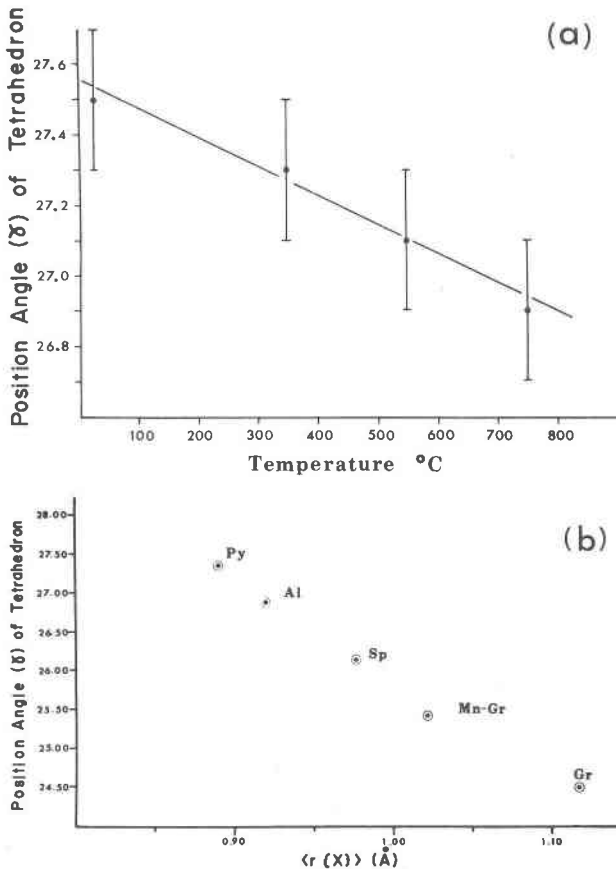
positional angle for the tetrahedron in pyrope decreases steadily from 27.5(2)° to 26.9(2)° over the temperature range 25° to 750°C (Fig. 2a), while no tetrahedral rotation occurs in grossularite. The consequences of this rotation will be discussed in a later section.

Al-Octahedron

The Al-octahedron in garnet is quite regular, as indicated by its small octahedral bond-angle strain (Robinson, Gibbs, and Ribbe, 1971). Nevertheless, an interesting contrast exists between the distortion of the Al-octahedron in pyrope and grossularite. The octahedron shares six of its twelve edges with adjacent triangular dodecahedra while the other six edges remain unshared. The shared edge, O(1)–O(4), at 25°C is shorter in pyrope (Fig. 1) than the unshared edge, O(1)–O(5), by 0.10 Å, as would be predicted by Pauling's electrostatic bonding principles (1929). In grossularite, however, the shared edge is 0.03 Å longer than the unshared edge.

Figure 3 illustrates the response of the shared and unshared octahedral edges to heating. In pyrope the expansion of the shared edge is almost an order of magnitude larger than that of the unshared edge (Table 7) whereas in grossularite both edges expand at approximately the same rate. The difference in the expansion rates of the two edges in pyrope causes the octahedral bond-angle strain to decrease with increasing temperature. The octahedral bond-angle strain is known to decrease in the aluminum silicate garnets in going from pyrope to Mn-grossularite as a

FIG. 2. Tetrahedral position angle (γ) *versus:* (a) temperature for pyrope, (b) $\langle r\{X\} \rangle$ for the aluminum silicate garnets pyrope (Py), almandine (Al), spessartine (Sp), Mn-grossularite (Mn-Gr), and grossularite (Gr). Data from Novak and Gibbs (1971).
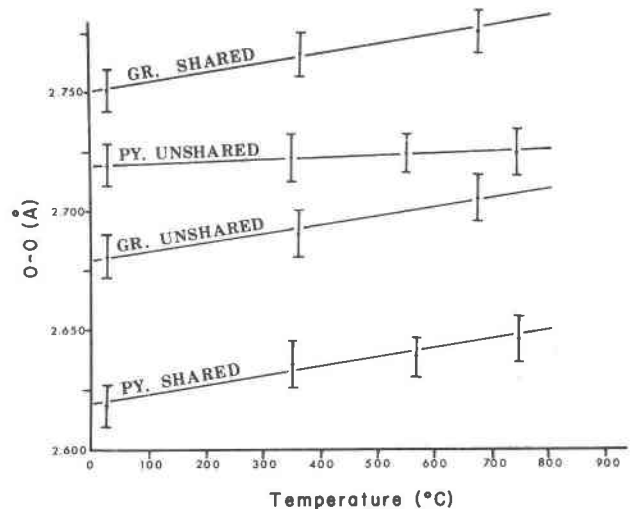
FIG. 3. A plot of the shared and unshared octahedral edge lengths *versus* temperature for pyrope and grossularite.

result of the increased radius of the *X*-cation (Novak and Gibbs, 1971).

Figure 4a illustrates the linear increase in the Al–O distance with increasing temperature in pyrope and grossularite. The thermal expansion of the Al–O interatomic distance in grossularite $1.3 \times 10^{-5}/°C$ is slightly greater than that of pyrope, $7.9 \times 10^{-6}/°C$.

Triangular Dodecahedron

There are two symmetrically non-equivalent {*X*}–O interatomic distances in the eight-coordinated triangular dodecahedron. Consideration of the cation-cation repulsion across the edge shared with the Si-tetrahedron would lead one to believe the *X*(1)–O(4) distance should be longer than the *X*(2)–O(4) distance (Fig. 1), whereas the reverse is actually true for all silicate garnets analyzed to date. Zemann (1962) and Gibbs and Smith (1965) have proposed that the *X*(2)–O(4) distance is greater for geometric reasons. If it were the shorter distance, unreasonable [*Y*]–O and unshared octahedral edge distances would result.

In pyrope the Mg(2)–O(4) distance increases in length at a greater rate with increasing temperature than does the Mg(1)–O(4) distance, whereas in grossularite both Ca–O distances increase at an equal rate (Table 7). Mean Ca–O and Mg–O interatomic distances are plotted *versus* temperature in Figure 4b. The linear thermal expansion coefficients for the mean Mg–O and Ca–O interatomic distances
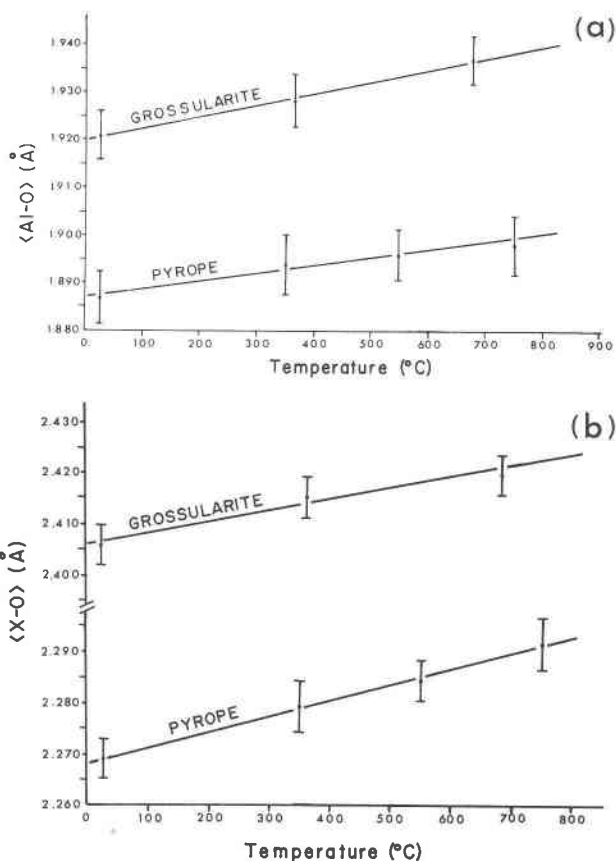
FIG. 4. (a) Variation of the mean Al–O interatomic distance with temperature. (b) Variation of the mean {*X*}–O interatomic distance with temperature.

in pyrope and grossularite are $1.3 \times 10^{-5}/°C$ and $8.3 \times 10^{-6}/°C$, respectively.

In pyrope the isotropic equivalent of the anisotropic thermal vibration parameters for Mg is greater at all temperatures than that for oxygen (see Table 2). Zemann and Zemann (1961) have suggested that positional disorder of the Mg contributes to the large apparent thermal vibration. Gibbs and Smith (1965) have attributed the larger *B*-value to the fact that Mg occupies a cavity larger than normal and that it tends to fill the cavity with a strong asymmetric vibration. Difference Fourier maps calculated through the Mg position for all the pyrope analyses in this study failed to substantiate the idea of positional disorder.

The rate of increase of the equivalent isotropic temperature factor with temperature—d*B*/d*T*—for the {*X*} cations (Fig. 5) is $2.0 \times 10^{-3} Å^2/°C$ for Mg in pyrope but $1.2 \times 10^{-3} Å^2/°C$ for Ca in grossularite. The refinements reveal that d*B*/d*T* for Mg is greater than that for Al or Si in pyrope whereas d*B*/d*T*

TABLE 7. Mean Thermal Expansion Coefficients (α) of Interatomic Distances* and Rates of Increase of Isotropic Temperature Factors**

	Pyrope	Grossularite
Mean Thermal Expansion Coefficients (α) x 10^5/°C		
X–O	1.3	0.8
Al–O	0.8	1.3
Si–O	0.1	0.7
d*B*/d*T* x 10^3 Å^2/°C		
X	2.0	1.2
Al	0.9	0.8
Si	0.6	1.1
O	1.3	1.2

* See text for explanation.
** $(B_T - B_{25°})/(T - 25°)$ was determined by linear regression.
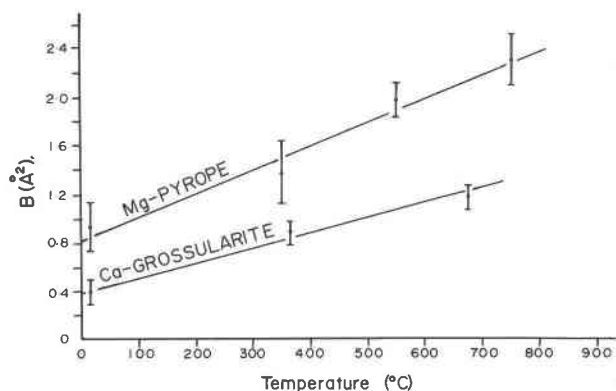
FIG. 5. A plot of the isotropic equivalent of the anisotropic temperature factor against temperature for Mg in pyrope and Ca in grossularite.

values for Ca, Al, and Si are approximately equal in grossularite (Table 7).

Comparison of Structural Changes as a Function of Heating and of Chemical Substitution

Novak and Gibbs (1971) observed certain trends in structure variations in the $\{X_3\}$ $[Al_2]$ (Si_3) O_{12} garnets as a function of the radius of the $\{X\}$ cation. The structural changes which occur in pyrope as a function of heating in some ways parallel those changes which would occur as a result of successive increases in the mean $\{X\}$–O distance through chemical sub-
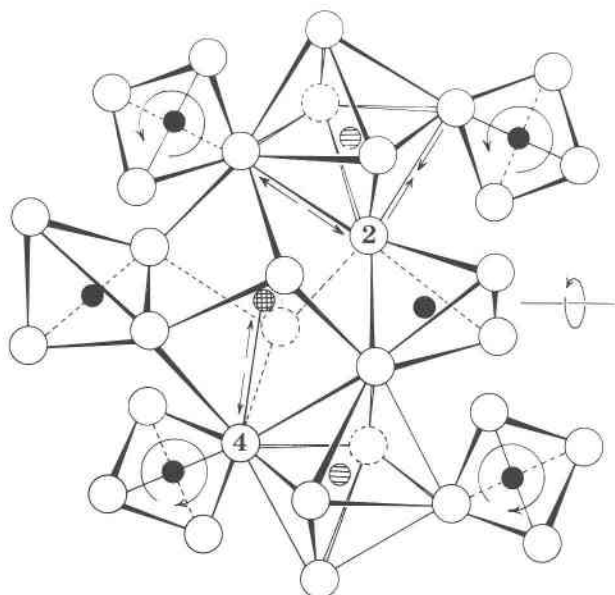

FIG. 6. A portion of the garnet structure showing the effect that rotation of the tetrahedra has on the relative lengths of the $[Al]O_6$ and $\{X\}O_8$ polyhedral edges. The tetrahedra are shown rotating to smaller γ values. Note the greater increase in the $\{X\}$–O(4) distance compared to $\{X\}$–O(2) with tetrahedral rotation.

stitution. For example, just as the tetrahedra in pyrope rotate to smaller tetrahedral position angles with increasing temperature, a similar rotation occurs in $\{X_3\}[Al_2](Si_3)O_{12}$ garnets as a mean radius of the $\{X\}$ cation increases (Fig. 2b). In the garnet structure a rotation of the tetrahedron about the $\bar{4}$ axis in a direction of decreasing γ in effect increases the size of the triangular dodecahedron (Fig. 6). Furthermore, the rotation of the tetrahedron about the $\bar{4}$ axis will lengthen the $X(2)$–O(4) distance at a greater rate than $X(1)$–O(4). This trend is observed in the pyrope structure with increasing temperature (Table 5). In the $\{X_3\}[Al_2](Si_3)O_{12}$ garnets with the mean radius of $\{X\}$, $\langle r\{X\}\rangle$, increasing from 0.89 to 1.12 Å, the $X(1)$–O(4) distance increases 0.12 Å while $X(2)$–O(4) increases 0.15 Å (Novak and Gibbs, 1971). The $X(1)$–O(4) increase is somewhat greater than rotation alone would allow because the shared edge of the tetrahedron also lengthens with increasing $\langle r\{X\}\rangle$.

Novak and Gibbs also showed that the octahedral distortion in the aluminum silicate garnets decreases as $\langle r\{X\}\rangle$ increases from 0.89 Å to 1.01 Å. At a radius of 1.01 Å, the shared and unshared octahedral edges are approximately equal in length. The aluminum octahedron in pyrope responds similarly to increasing temperature, becoming less distorted as its shared octahedral edge increases in length at a greater rate with increasing temperature than does its unshared edge (Fig. 3).

The parallelism of pyrope's response upon heating to substitution of a larger $\{X\}$ cation may be due in part to the fact that dB/dT for Mg is greater than for the remaining cations and, therefore, has a greater effective radius at higher temperatures. This cannot be said for Ca in grossularite since dB/dT for Ca is approximately equal to that for Al and Si (Table 7).

To aid in the understanding of the response of the $\{X_3\}[Al_2](Si_3)O_{12}$ garnet structure to heating or to chemical substitution in the triangular dodecahedral site, the computer program, Distance Least-Squares (DLS), written by Meier and Villiger (1969) was utilized. In the program, atomic positional parameters are determined by means of least-squares optimization of interatomic distances to prescribed distances. In this analysis the intent was not to "synthesize" a given garnet structure, but rather to determine trends in the response of the Al-silicate garnet structure to $\{X\}$ cations of various radii. In an attempt to keep the analysis as bias-free as possible, the prescribed cation-oxygen distances were taken as the sum of the Shannon and Prewitt (1969) radii for the appropriate coordination, and the O–O distances about each

polyhedron were calculated from each metal-oxygen distance assuming an undistorted polyhedron (Drits, 1971). The cell edges used were calculated from the Novak and Gibbs (1971) equation relating cell edge to radii of the $\{X\}$ and $[Y]$ cations.

In the refinements the prescribed interatomic distances were weighted proportional to their calculated valence bond strength such that weights for the Si–O, Al–O, and X–O distances were 1.0, 0.5, and 0.25, respectively (Pauling, 1929). Unless otherwise stated the O–O distances were given a weight of 0.07 following Baur (1971). If the weights are chosen correctly, this type of analysis approximates a simple ionic force model. Cation-cation and anion-anion repulsions are considered only through the prescribed interatomic distances and associated weights.

A series of refinements were carried out with the $\{X\}$ cation radius varying from 0.89 Å (Mg) to 1.12 Å (Ca). With weights of 0.07 for the oxygen-oxygen distances in the initial refinements it was discovered that unlikely O–O distances resulted. For example, in all the refinements the unshared triangular dodecahedral edge O(4)–O(7) refined to less than 2.67 Å even though the prescribed value ranged from 2.75 Å for pyrope to 2.89 Å for grossularite (Table 8). Zemann (1962) likewise found in his calculations for an "ideal garnet" that this edge was far too short and con-

cluded that in the aluminum silicate garnets this distance could be no shorter than 2.75 Å. In addition, in the DLS calculations the unshared octahedral edge O(1)–O(5) refined from the prescribed distance of 2.70 Å to values less than 2.68 Å for garnets where r $\{X\}$ exceeded 1.0 Å. Novak and Gibbs (1971) have proposed that 2.68 Å is a lower limit for the unshared octahedral edge in silicate garnets.

In an attempt to account for O–O interaction the unshared triangular dodecahedral edge and the unshared octahedral edge were given prescribed distances of 2.75 and 2.68 Å, respectively, in the structures where these limits were exceeded. In addition, these distances were given weights of 1.0 in the refinement, equivalent to the weight of the Si–O distance. The final refined bond lengths for pyrope and grossularite are given in Table 8.

Certain trends became apparent from the distance least-squares refinements. First, the $X(2)$–O(4) distance always refined to values larger than the $X(1)$–O(4) distance. This is consistent with determined distances in all silicate garnets analyzed to date and confirms Zemann's contention that the $X(2)$–O(4) distance must be longer because of structural constraints. Secondly, the shared tetrahedral edge refined to a smaller value than the unshared edge in all cases without cation-cation repulsion be-

TABLE 8. Distance Least-Squares Results for Pyrope and Grossularite

	PYROPE a_{calc} = 11.474 Å			GROSSULARITE a_{calc} = 11.840 Å		
	Prescribed distance	Refined distance	Observed[*] distance	Prescribed distance	Refined distance	Observed[*] distance
Si–O	1.64 Å	1.64 Å	1.634(1) Å	1.64 Å	1.64 Å	1.645(1) Å
Al–O	1.91	1.90	1.886(1)	1.91	1.93	1.924(1)
X(1)–O(4)	2.27	2.21	2.196(2)	2.50	2.37	2.319(1)
X(2)–O(4)	2.27	2.32	2.342(2)	2.50	2.46	2.490(1)
shared octahedral edge						
O(1)–O(4)	2.70	2.63	2.617(3)	2.70	2.79	2.756(2)
unshared octahedral edge						
O(1)–O(5)	2.70	2.75	2.716(2)	2.70	2.67[**]	2.686(2)
shared tetrahedral edge						
O(1)–O(2)	2.68	2.52	2.494(2)	2.68	2.62	2.567(2)
unshared tetrahedral edge						
O(1)–O(3)	2.68	2.76	2.751(3)	2.68	2.71	2.745(1)
unshared tri. dodec. edge						
O(4)–O(7)	2.75	2.75[†]	2.782(3)	2.89	2.75[†]	2.866(1)

[*]   Novak and Gibbs (1971).
[**] Weight of 1.0 given to prescribed O–O distance at 2.68 Å.
[†]   Weight of 1.0 given to prescribed O–O distance at 2.75 Å.

ing considered in the refinement. This is not to say that cation-cation repulsion has no influence on the length of the shared edge, but rather that such repulsion is not the only factor in determining that the shared edge will be shorter than the unshared edge in the garnet structure (cf Born and Zemann, 1964). Thirdly, for increasing values of X–O distances, the refinements show a continuous trend in which the unshared octahedral edge length decreases to the proposed 2.68 Å limit while the shared edge length increases. As shown in Table 8, the two octahedral edges refine to values in pyrope such that the shared edge is shorter than the unshared edge whereas the reverse occurred in the grossularite refinement. This suggests that the increase in the shared octahedral edge in $\{X_3\}[Al_2](Si_3)O_{12}$ garnets, as the radius of the $\{X\}$ cation increases, is more a consequence of structural constraints than of decreased cation-cation repulsion between the $\{X\}$ cation and [Al] as has been proposed by previous investigators.

In pyrope, although the unshared octahedral edge does not actually decrease as a function of temperature (due to the thermal expansion of the unit cell) its coefficient of expansion is significantly smaller at $7.4 \times 10^{-6}/°C$ than is that of the shared edge at $3.6 \times 10^{-5}/°C$. The unshared octahedral edge in grossularite at 25°C is 2.681 Å which, as previously mentioned, appears to represent a lower limit. This distance increases linearly with increasing temperature to 2.705 Å at 675°, which probably represents the lower limit of an unshared octahedral edge at that particular temperature for a silicate garnet, bearing in mind that corrections for thermal displacements have not been made.

The distance least-squares refinements reveal that the Al–O distance remains fairly constant with increasing $r\{X\}$ up to the point where the unshared octahedral edge reaches the 2.68 Å limit, whereupon the Al–O distance begins to increase with further increase of $r\{X\}$. This is consistent with the observed difference in the thermal expansion of the Al–O interatomic distance in pyrope as compared to grossularite. In pyrope where the unshared octahedral edge at 25°C is 2.719 Å, the α(Al–O) is $7.9 \times 10^{-6}/°C$. The α(Al–O) in grossularite, where the shared edge at 25°C is 2.681 Å, is somewhat higher at $1.3 \times 10^{-5}/°C$.

Although certain trends in the variation of the SiO_4–AlO_6 polyhedral framework brought about by chemical expansion of the XO_8 triangular dodecahedron are similar to those resulting from thermal expansion, the effects of the two mechanisms on the details of the garnet structure are different. For example, an increase in $\langle r\{X\}\rangle$ of 0.03 Å above that for pyrope causes the mean $\{X\}$–O and [Al]–O distances to increase by 0.031 Å and 0.010 Å, respectively, while the unshared O–O edges of both the tetrahedron and octahedron decrease in length (Novak and Gibbs, 1971). Heating of pyrope to 750°C causes the mean $\{X\}$–O and [Al]–O distances to increase 0.023 Å and 0.010 Å, respectively, and the unshared O–O edges of the tetrahedra and octahedra show no statistically significant change in length.

Based upon the response of the pyrope and grossularite structures to heating, one might speculate as to the structural variations an aluminumsilicate garnet with $r\{X\}$ intermediate to Mg and Ca might show with increasing temperature. For instance, if the response of the SiO_4–AlO_6 framework to increasing temperature is influenced by the size of the $\{X\}$ cation, one might predict that mean thermal expansion coefficient for the [Al]–O distance would be intermediate to that in pyrope and grossularite. Likewise, the tetrahedron in these intermediate garnets would be expected to rotate to smaller values of γ as a function of temperature and would possess successively lower $d\gamma/dT$ values as $\langle r\{X\}\rangle$ increases. In an attempt to provide further information regarding the high temperature crystal chemistry of silicate garnets, crystal structure investigations of spessartine and andradite at elevated temperatures are planned.

References

ABRAHAMS, S. C., AND S. GELLER (1958) Refinement of the structure of a grossularite garnet. *Acta Crystallogr.* **11**, 437–441.

BAUR, W. H. (1971) Geometric refinement of the crystal structure of β-Mg_2-SiO_4. *Nat. Phys. Sci.* **233**, 135–137.

BORN, L., AND J. ZEMANN (1964) Abstandsberechnungen und gitterenergetische Berechnungen an Granaten. *Contrib. Mineral. Petrol.* **10**, 2–23.

BROWN, G. E., AND C. T. PREWITT (1973) High-temperature crystal chemistry of hortonolite. *Am. Mineral.* **58**, 577–587.

BUSING, W R., K. O. MARTIN, AND H. A. LEVY (1962) ORFLS: A Fortran crystallographic least-squares refinement program. U.S. *Nat. Tech. Inform. Serv.*, ORNL-TM-**305**.

——, ——, AND —— (1964) ORFFE: A Fortran crystallographic function and error program. U.S. *Nat. Tech. Inform. Serv.*, ORNL-TM-**306**.

CRUICKSHANK, D. W. J. (1965) Errors in least-squares methods. In J. S. Rollett, Ed., *Computing Methods in Crystallography.* Pergamon Press, New York, p. 112–116.

DOYLE, P. A., AND P. S. TURNER (1968) Relativistic Hartree-Fock X-ray and electron scattering factors. *Acta Crystallogr.* **A24,** 390–397.

DRITS, V. A. (1971) The relationship between the average anion-anion and anion-cation distances in the simplest crystal structure units: tetrahedra and octahedra. *Soc. Phys. Crystallogr.* **15,** 795–798.

EULER, FERDINAND, AND JANE A. BRUCE (1965) Oxygen coordinates of compounds with garnet structures. *Acta Crystallogr.* **19,** 971–978.

FOIT, F. F., AND D. R. PEACOR (1967) A high temperature furnace for a single crystal X-ray diffractometer. *J. Sci. Instrum.* **44,** 183–185.

GELLER, S. (1967) Crystal chemistry of the garnets. *Z. Kristallogr.* **125,** 1–47.

GIBBS, G. V., AND J. V. SMITH (1965) Refinement of the crystal structure of synthetic pyrope. *Am. Mineral.* **50,** 2023–2039.

MEAGHER, E. P. (1973) The crystal structures of grossularite and pyrope garnet at high temperatures (abstr.). *Geol. Soc. Am. Abstr. Program,* **5,** 735.

MEIER, VON W. M., AND H. VILLIGER (1969) Die Methode der Abstandsverfeinerung zur Bestimmung der Atomkoordinaten idealisierter Gerustsrukturen. *Z. Kristallogr.* **129,** 411–423.

MENZER, G. (1926) Die Kristallstrukture von Granat. *Z. Kristallogr.* **63,** 157–158.

NELSON, J. E., AND D. P. RILEY (1945) An experimental investigation of extrapolation methods in the derivation of accurate unit-cell dimensions of crystals. *Proc. Phys. Soc. (London),* **57,** 160–177.

NOVAK, G. A., AND G. V. GIBBS (1971) The crystal chemistry of the silicate garnets. *Am. Mineral.* **56,** 791–825.

———, AND HENRY O. A. MEYER (1970) Refinement of the crystal structure of a chrome pyrope garnet: An inclusion in natural diamond. *Am. Mineral.* **55,** 2124–2127.

PAULING, L. (1929) The principles determining the structure of complex ionic crystals. *J. Am. Chem. Soc.* **51,** 1010–1026.

PRANDL, WOLFRAM (1966) Vereinerung der Kristallstrukture des Grossulars mit Neutronen und Rontgenstrahlbeugung. *Z. Kristallogr.* **123,** 81–116.

ROBINSON, K., G. V. GIBBS, AND P. H. RIBBE (1971) Quadratic elongation: A quantitative measure of distortion in coordination polyhedra. *Science,* **172,** 567–570.

SHANNON, R. D., AND C. T. PREWITT (1969) Effective ionic radii in oxides and fluorides. *Acta Crystallogr.* **B25,** 925–946.

SKINNER, B. J. (1956) Physical properties of end-members of the garnet group. *Am. Mineral.* **41,** 428–436.

SMYTH, J. R., AND R. M. HAZEN (1973) The crystal structures of forsterite and hortonolite at several temperatures up to 900°C. *Am. Mineral.* **58,** 588–593.

ZEMANN, A., AND J. ZEMANN (1961) Verfeinerung der kristallstruktur von synthetischeim pyrope, $Mg_3Al_2(SiO_4)_3$. *Acta Crystallogr.* **14,** 835–837.

ZEMANN, F. (1962) Zur Kristallchemie der granat. *Beitr. Mineral. Petrol.* **8,** 180–188.